Macromolecules
ARTICLE

Macromolecules **2009**, *42*, 5717–5727 **5717**
DOI: 10.1021/ma9008109

Analysis of the C=O Stretching Band of the α-Crystal of Poly(L-lactide)

E. Meaurio, I. Martinez de Arenaza, E. Lizundia, and J. R. Sarasua*

School of Engineering, University of the Basque Country (EHU-UPV), Alameda de Urquijo s/n, 48013 Bilbao, Spain

Received April 14, 2009; Revised Manuscript Received June 4, 2009

ABSTRACT: The C=O stretching band of the α-crystal of PLLA has been investigated. In the α crystals splitting reveals the existence of an ordered arrangement of transition moments in the different sites along the helical chain of PLLA. In the α′ crystals splitting is not observed denoting a lack of ordered arrangement in transition moments. In the α crystals the band at 1776 cm^{-1} arises from the A mode, and because of its low intensity, its profile is barely changed by transition dipole coupling (TDC) interactions. The E_1 mode is centered at about 1759 cm^{-1}, and is strongly split due to TDC interactions (also referred as Davydov or exciton splitting) in the lateral direction, resulting in the broad absorption profile observed below 1776 cm^{-1} in the C=O stretching region. Five different sites (characterized by the arrangement of transition moments) can be discerned along the PLLA helix in the unit cell, each of them establishing TDC interactions of different strength with the chains in the first layer. The C=O stretching band can be regarded as a continuum of adjacent contributions, from which only the overall envelope is observed. The value obtained for the transition moment suggests that excitonic interactions may occur in a collective mode involving the five distinguishable C=O groups in PLLA, explaining the large splitting observed in the C=O stretching region of crystalline polylactides. Repulsive C=O dipole−dipole interactions have also been found, related to the symmetry of the unit cell.

Introduction

Biodegradable and biocompatible polymers such as poly(L-lactide) (PLLA) show interesting properties for biomedical[1] and packaging[2] applications and have attracted much attention, especially since the beginning of their commercial production. PLLA is a stereoregular crystalline polymer crystallizing in different polymorphs: α-,[3] β-,[4] or γ-form.[5] The β-form is only produced under a high drawing ratio,[4] and the γ-form is prepared by epitaxial crystallization under special substrates.[5] Crystallization of PLLA from the melt or solution under normal conditions results in its most common and stable polymorph, α-form, with a 10_3 helical chain conformation.[3] Solution grown crystals show a lozenge habit suggesting an orthorhombic unit cell, as in polyethylene.[6] According to diffraction experiments,[7] the dimensions of the unit cell are $a = 10.6$ Å, $b = 6.1$ Å, and $c = 28.8$ Å, suggesting nearly hexagonal packing of the chains according to the ratio of axis lengths, $a/b \approx 3^{1/2}$. In fact, Kalb and Pennings[8] proposed a hexagonal unit cell for PLLA from electron diffraction experiments. In addition, hexagonal morphologies have been observed for solution grown[6] and melt crystallized lamellae,[9] being attributed to an almost hexagonal packing of the chains in the orthorhombic unit cell.[6−9]

Ohtani[10] and Yasuniwa[11] suggested the formation of the β-form polymorph during crystallization in the low temperature range, and attributed to the new polymorph the distinct characteristics of these crystals. This hypothesis was later discarded by Zhang et al.[12] because of the lack of the characteristic infrared band of PLLA β-crystals at about 908 cm^{-1}.[12−15] In addition, Zhang et al.[12] suggested the existence of a new polymorph, α′, to explain the differences observed mainly in the IR spectrum between samples crystallized below and above 120 °C. The new polymorph would consist on chains packed in a 10_3 helical conformation and would only differentiate from the α-form polymorph in the lateral packing of the chains.

At present, several aspects of the crystalline structure of PLLA remain unclear. For example, Aleman et al.[16] and Sasaki et al.[17] have proposed different coordinates for the atoms in the unit cell of the α-form. The α′-form is even more elusive to structural analysis because it shows extremely simple diffraction patterns.[12,18] It is reported to be a "disordered crystal" with a loose packing in the lateral direction[12] and to crystallize in a pseudohexagonal unit cell.[18] Infrared spectroscopy can be a valuable tool to gain insight in the crystalline structure of polymers; in fact, the existence of the new polymorph α′ was proposed in view of the noticeable differences in the FTIR spectrum of the two polymorphs.[12] Specifically, the C=O stretching band of α-form shows complex splitting, but the same band for the α′-form displays a simple profile. The origin of the different spectral profiles is not understood because the origin of the complex splitting in the C=O stretching band of the α-crystals is still unclear, as the split components have not been related to specific vibrational modes.

Spectroscopic techniques are of key importance to investigate the structure of materials. In this regard, the structure of the crystalline phase in PLLA determines the physical, chemical, and mechanical properties of the bulk material. FTIR spectroscopy is usually used for identification purposes, but this technique can also provide information specific to the crystalline phase when intermolecular interactions exist.[28] In fact, FTIR spectroscopy has been widely used to complement the information obtained by diffraction analyses and is also used as a fast, non destructive tool for the determination of the crystallinity of polymer samples.[28] Among the different bands amenable to spectral analysis, the C=O stretching band is the most important because it is a localized vibrational mode, almost uncoupled from the vibrational modes of the chain skeleton, and usually well resolved in the infrared spectrum. However, the effects of intermolecular

*Corresponding author. E-mail: jr.sarasua@ehu.es.

Published on Web 07/09/2009

interactions and the mechanisms of absorption of radiation can complicate this infrared region. It is therefore necessary to understand the origin of the spectral components observed in the C=O stretching band to extract the information provided by this region.

This paper provides a vibrational analysis of the C=O stretching band of α-crystals, relating the complex spectral profile of the α-crystals of PLLA with its crystalline structure. Unfortunately, the literature dealing with spectral splitting can be confusing because the same term can be used by different authors to refer to different phenomena.[19−22] In this paper, the terminology of ref 22 is adopted, classifying the splitting mechanisms as follows:

- Site (Group) Splitting or Crystal Field Splitting. Splitting arising from the static intermolecular forces in the crystal. Can occur when molecules occupy more than onetype of crystal site or when molecules lay on a crystal site of lower symmetry than that of the gaseous molecule. Usually, the term "crystal field splitting" refers specifically to the latter case.
- Correlation (Field) Splitting, Davydov Splitting, or Exciton Splitting. Splitting arising from the dynamic-intermolecular forces in the crystal. Occurs owing to intermolecular vibrational coupling.
- Factor Group Splitting or Unit Cell Group Splitting. The combined effect of site splitting and Davydov splitting in the spectra of crystals.

According to the analysis of the C=O stretching band of PLLA performed in this paper, splitting is attributed to Davydov splitting in the five interacting sites located along the PLLA helix in the unit cell. In addition, the contribution of C=O dipole−dipole interactions is repulsive.

Experimental Part and Methods

A. Starting Materials. Optically pure poly(L-lactide) containing less than 0.01% of residual solvent and less than 0.1% residual monomer was supplied by *Purac Biochem* (The Netherlands). Its specific rotation in chloroform at 20 °C was −157.3°. The molecular weight of poly(L-lactide) was measured viscometrically in a Ubbelohde type viscometer in chloroform at 30 °C, using the relation:[23]

$$[\eta] = 5.45 \times 10^{-4} M_v^{0.73} (\mathrm{dL/g}) \quad (1)$$

A value of $M_v = 3.2 \times 10^5$ g/mol was obtained.

B. Infrared Spectroscopy. Infrared spectra of PLLA films were recorded on a Nicolet AVATAR 370 Fourier transform infrared spectrophotometer (FTIR). Typical samples were prepared by spreading two drops of a 0.8 wt % PLLA solution over 13 mm diameter KBr pellets. The solution was allowed to evaporate at room temperature followed by vacuum drying at 50 °C for 48 h. Resulting polymer films were completely amorphous and the absorbance was 0.5 ± 0.2 units (film thickness 0.7 μm ± 0.3).[24] Thermal treatments were performed in a temperature cell accessory controlled within an accuracy of ±1 °C.

The isothermal cold crystallization experiment was carried out heating at 10 °C/min to 80 °C and isothermally crystallizing to completion (1 h). Isothermal crystallization from the melt was performed by heating at 10 °C/min to 200 °C, maintaining for 5 min to melt completely, and then cooling at 5 °C/min to 160 °C and isothermally crystallizing for 60 h to achieve a high crystallinity film. Samples were then cooled slowly to obtain the room temperature spectrum. In all cases spectra were recorded by coadding 32 scans at a 2 cm^{-1} resolution.

The crystallinity of the PLLA samples has been measured using an amorphous band located at 955 cm^{-1}, assigned to CH_3 rocking coupled with skeletal C−C stretching in the amorphous phase.[25] When PLLA crystallizes in 10_3 helical conformation, the $r_{CH_3} + \nu_{CC}$ mode shifts to 920 cm^{-1}, leaving the amorphous and crystalline contributions almost completely resolved, and the crystallinity of the samples can be easily calculated according to[13,24,26]

$$X_c = \frac{I_{955}^0 - I_{955}}{I_{955}^0} \quad (2)$$

where I_{955}^0 and I_{955} are, respectively, the room temperature intensities (integrated absorbance or area) before and after crystallization. The intensity of this band shows temperature dependence and thermal history dependence in the glassy state. To avoid errors in the determination of the crystallinity using eq 2, the initial and final intensities must be obtained from samples with the same thermal history. For this purpose, the as cast samples were first heated to 72 °C (just above the T_g of the sample, 70 °C),[27] maintained for 5 min, and allowed to cool to room temperature to obtain the room temperature spectrum of the amorphous sample cooled from the rubbery state (I_{955}^0).

Results and Discussion

In principle, infrared spectroscopy is sensitive to the conformational state of molecules, but not to the crystalline order.[20,28,29] Therefore, in most cases the spectrum of a pure crystalline phase (obtained by subtraction of the spectrum corresponding to the amorphous phase) only reflects the spectrum of single chains with the crystalline conformation.[20,28] However, IR spectroscopy also provides information about the crystalline phase through its sensitivity to interactions and the occurrences of site splitting, correlation splitting and factor group splitting phenomena.[22,30−32]

A. Background on the C=O Stretching Region of Amorphous PLLA. The conformational sensitivity of the C=O stretching band must be recalled[33] before attempting the analysis of the spectral changes observed in crystalline samples. As can be seen in Figure 1, the second derivative

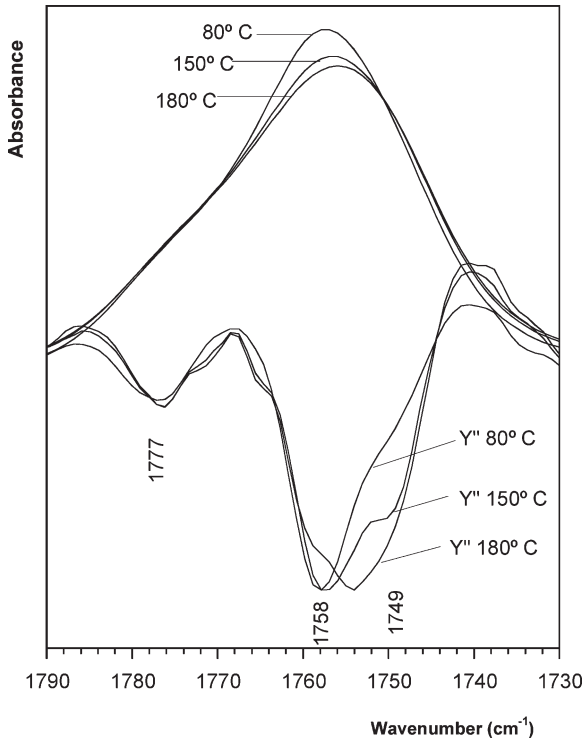

Figure 1. Top side: Spectra in the C=O stretching region of amorphous PLLA at different temperatures. Bottom side: Autoscaled second derivative spectra.

of the C=O stretching band of amorphous PLLA displays three different components. The splitting of amorphous PLLA can not be attributed to specific C=O···H−C interactions because these have been discarded from the analysis of the C−H stretching band.[34] Traditionally, splitting in polypeptides of alanyne and glycine (with chemical structure similar to PLLA) has been explained assuming transition dipole coupling (TDC) interactions, consisting in the electrostatic coupling of point dipoles.[35] However, even though TDC interactions can explain band splitting in ordered arrangements (protein helical forms and sheets), in amorphous systems only band broadening can be expected from dipole−dipole interactions, because there is continuum of attractive and repulsive interactions of variable strength depending on distance and orientation between dipoles.[36] In addition, Torii et al.[37] reported substantially larger coupling interactions for isolated di- and tripeptides using ab initio methods compared to the values calculated using TDC interactions alone, concluding the existence of through-bond interactions. These are considered next-neighbor interactions and currently the spectra of polypeptides is being revisited using ab initio methods to calculate the interaction between adjacent peptide units and TDC interactions to account for through space coupling.[38−41] The through-bond interaction can be also expected in PLLA, because enhanced splitting in the C=O stretching band is a general behavior when atoms with unshared electron pairs (such as nitrogen and oxygen) are located between the C=O groups.[33,42] Therefore, through bond interactions in PLLA (consisting in the intramolecular interaction between the C=O groups located in adjacent units), provide an explanation for the local sensitivity to conformation in the PLLA chain.[33] The breadth of each of the components in Figure 1 should be related to the dispersion of the dipole−dipole interactions.[36]

The conformational analysis of PLLA was performed by Brant et al.[43] Three skeletal bonds occur along the molecular chain in poly(L-lactide): C−O (ester), O−C_α, and C_α−C. The C−O (ester) bond was assumed to be always trans due to conjugation with the C=O double bond. Two energy minima were obtained for the O−C_α bond around −160° and −73°, and another two for the C_α-C bond around 160° and −48°. Therefore, four minimum energy states exist corresponding to four distinct conformations for the O−C_α and C_α−C bonds: tt (−160°, 160°), tg (−160°, −48°), gt (−73°, +160°), and gg (−73°, −48°). All these conformers form helical chains, and the gt (10_3 helix) has the lowest energy. Regular helix models of these conformers were built.[33] For gg conformers, the C=O groups are nearly parallel to the helical chain, and absorption was predicted only for the vibrational mode with phase angle $\delta = 0°$. The remaining conformers, tg, gt, and tt, form 5_1, 10_3, and 2_1 helixes respectively with the C=O groups oriented nearly perpendicular to the helical chain. Therefore, absorption is predicted for the vibrational modes with $\delta = 72°$, 108° and 180° respectively. In the frame of the Miyazawas first order perturbation theory,[35] and assuming only intramolecular coupling with nearest neighbors, the absorption wavenumbers corresponding to the amorphous components (1777, 1758, and 1749 cm^{-1}) showed a very good correlation with the phase angles corresponding to gg, gt and tt conformers (0°, 108°, and 180°) so that the following equation was proposed for the through bond interactions:[33]

$$\tilde{\nu}(\boldsymbol{\delta}) = 1763 + 14\cos(\boldsymbol{\delta}) \quad (3)$$

where $\tilde{\nu}(\delta)$ is the absorption wavenumber, 1763 cm^{-1} is the unperturbed frequency, and 14 cm^{-1} is the perturbation parameter. According to eq 3, gg, tg, gt, and tt conformers absorb respectively at 1777, 1767, 1759, and 1749 cm^{-1}. The contribution corresponding to tg conformers is not observed in Figure 1 probably due to their high relative energy.

Finally, note that eq 3 was obtained by fitting the amorphous components with the absorbing phase angles obtained from regular helix models, and this procedure relies on the likely persistence of the helical structures for a number of residues in the amorphous phase.[55] In addition, eq 3 is supported by the following experimental evidences: (i) it provides a natural explanation and a good fit for the components obtained in the amorphous phase, (ii) relative areas of the peaks agree with the relative population of the conformers, and (iii) the perturbation parameter is in very good agreement with that obtained for the monomeric unit L-lactide (LLA), D_{LLA} = 15 cm^{-1}.[24] Note that even if a certain error was introduced on adopting the wavenumbers measured for the conformers in the amorphous phase to fit the phase angles corresponding to regular helixes, this error should hardly invalidate the identification of the conformers, which in fact is the main result necessary to deal with the analysis of the spectrum of the crystalline phase.

B. The C=O Stretching Region of Crystalline PLLA. Figure 2a displays the spectra in the C=O stretching region of PLLA recorded during isothermal crystallization from the melt at 160 °C (α crystals). As can be seen, four new contributions apparently located at about 1776, 1767, 1759, and 1749 cm^{-1} can be resolved according to the second derivative spectrum, which should be attributed to the crystalline phase (gt conformers) due the narrow profile of the derivative peaks.[19] The dependence of intensity on crystallization progress in the crystalline spectrum of Figure 2a can be easily explained considering the evolution of the amorphous contributions (Figure 1). For example, the crystalline contribution at 1749 cm^{-1} seems important according to the second derivative spectrum, but the absorbance at this location barely increases during crystallization. This is because amorphous tt conformers (absorbing at 1749 cm^{-1}) are also consumed during the ordering process. The absorbance at 1776 cm^{-1} decreases in spite of the new crystalline component at that location. This can be attributed to the reduction of the population of amorphous gg conformers, not compensated by the low intensity crystalline component occurring at this location.

Figure 2b displays the spectra in the C=O stretching region of PLLA recorded during isothermal crystallization from the glassy state at 80 °C (α′ crystals). As can be seen, crystallization proceeds very fast and can be considered complete after short time. The crystallinity of this sample is however much smaller than that of the highly ordered sample crystallized from the melt (46% vs 80%, measured from the amorphous band located at 955 cm^{-1}).[24] As can be seen, the sample crystallized from the melt displays complex splitting but the sample prepared by cold crystallization does not, even though in both cases PLLA crystallizes in the 10_3 helical conformation. Hence, splitting can not be attributed to intramolecular interactions (these should be similar in both samples), but to the regular crystalline structure obtained during crystallization at high temperatures. Actually the existence of different polymorphs termed α (crystallized above 120 °C, splitting is observed) and α′ (crystallized below 100 °C, splitting is not observed) has been proposed.[12]

The spectrum of the α′-form (Figure 2b) only displays a crystalline band located at about 1760 cm^{-1}, attributed to the E_1 mode (transition moment perpendicular to the helical chain). It can be regarded as the spectrum of a single helical chain because the splitting attributable to intermolecular

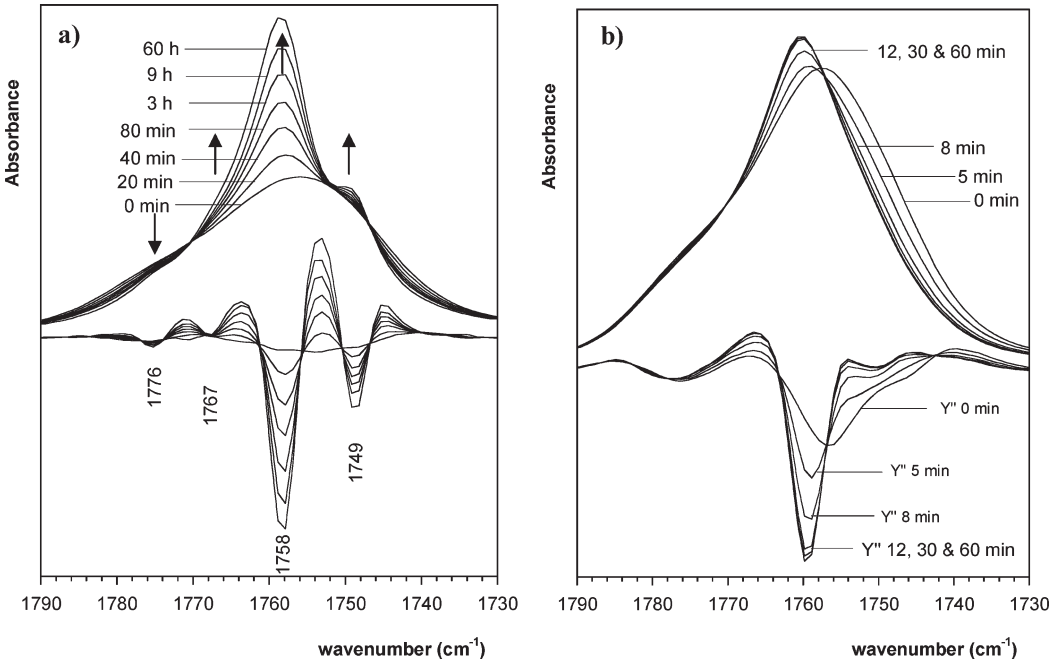

Figure 2. Carbonyl stretching region of PLLA (upper side spectra) and second derivatives (bottom side spectra) recorded during (a) isothermal crystallization from the melt at 160 °C and (b) isothermal crystallization from the glassy state at 80 °C. The arrows in part a indicate the variation of absorbance during crystallization.

interactions in ordered systems is not observed.[28] The intramolecular interactions can be analyzed in the frame of the Miyazawas first order perturbation theory:[35,44,45]

$$\tilde{\nu}(\boldsymbol{\delta},\boldsymbol{\delta}') = \tilde{\nu}_0 + \sum_{s,t} D_{st} \cos(s\boldsymbol{\delta}) \cos(t\boldsymbol{\delta}') \qquad (4)$$

where $\tilde{\nu}_0$ is the unperturbed frequency, D_{st} is the interaction constant between C=O groups separated by t chains and s groups along the ith neighboring chain and δ and δ' are the phase angles between the vibrations in the respective ester groups. For intramolecular interactions, $t=0$, only the A and E_1 modes are predicted:

$$A(0) \quad \tilde{\nu}(0) = \tilde{\nu}_0 + D_{10} + D_{20} + \ldots \qquad (5)$$

$$E_1\left(\frac{2\pi 3}{10}\right) \quad \tilde{\nu} = \tilde{\nu}_0 + D_{10}\cos\left(\frac{2\pi 3}{10}\right) + D_{20}\cos\left(2\frac{2\pi 3}{10}\right) + \ldots \qquad (6)$$

Similar equations have been also used to analyze the location of the A and E_1 mode bands in the α-helix of polypeptides[44,45] (using the appropriate phase angle for the perpendicular mode), and a parallel analysis can be performed. We will focus on the E_1 mode as the A mode is not observed for the PLLA sample crystallized at 80 °C. In case of polypeptides, the location of the amide I components was dominated by the D_{10} term, much larger than the consecutive D_{20} and D_{30} terms (the latter was actually enhanced because the interaction was transmitted through hydrogen bond coupling between polypeptides in different turns along the helix).[44] In case of PLLA, hydrogen bonding can be discarded according to the analysis of the C−H stretching band;[34] therefore, only the D_{10} term should be considered relevant. Hence, eq 6 takes the same form of eq 3 (for $\delta = 2\pi 3/10$), but the D_{10} terms in both equations include different interactions. In case of eq 3, D_{10} was obtained from the

Table 1. Correlation Table for the Infrared Active Bands in the C=O Stretching Region of PLLA α-Crystal, Adapted from Reference 19

Line Group	Site Group	Factor Group
C_{10}	C_2	D_2
		A (inactive)
1A	*1A*	$1B_1$
$1E_1$	*5B*	$5B_2$
		$5B_3$

locations corresponding to conformers observed in the amorphous phase. As in disordered phases dipole−dipole interactions broaden absorption bands but do not change their location,[37] the interaction constant $D_{10} = 14\ \text{cm}^{-1}$ of eq 3 includes only through bond interactions between nearest neighbors. However, in eq 6, D_{10} includes both through bond interactions and intramolecular TDC interactions in the crystalline 10_3 helical chains. Neighboring C=O groups in the 10_3 helix are rotated 108°, and because of the slightly antiparallel orientation dipole−dipole interactions should be slightly attractive and should shift the 1759 cm^{-1} band to lower wavenumbers. However, the location found for the cold crystallized gt conformers of PLLA (1760 cm^{-1}) shows a positive shift relative to the location observed in the amorphous phase. According to evidence reported in the following sections, the positive shift probably arises from weak repulsive intermolecular interactions between permanent C=O dipoles. Hence, the spectrum of the α′-form of PLLA can be regarded as the spectrum of the 10_3 helical conformation in which the effect of both intramolecular and intermolecular TDC interactions is not observed. The spectrum does not provide information about the 3D order in the crystals.

We will focus now in the analysis of the spectrum of the α form (Figure 2a). Table 1 is the correlation table for the

infrared active bands in the C=O stretching region of the PLLA α-crystal.[19] The 10_3 helix of PLLA belongs to the C_{10} line group symmetry, and for the isolated helical chain only one C=O stretching A mode and one C=O stretching E_1 mode can again be expected. When PLLA crystallizes into its orthorhombic form, chain site symmetry with respect to the entire crystal is only C_2, and the vibrational activity changes as predicted by the first two columns in table 1. As can be seen, the E_1 mode splits in five B modes, a consequence of the lower symmetry of the site compared to the helical chain. This can be understood considering that the perpendicular component of the transition moment of the helix can be oriented in five distinguishable directions within the sites of C_2 symmetry. Of course, splitting will only be observed in the IR spectrum if degeneracy is lost, i.e., if the interaction between permanent dipoles is strong enough to shift the absorption. One split component is expected for each site, and the splitting is known as site group splitting or crystal field splitting.[22]

Intermolecular interactions can couple the vibrational modes of the sites. For each site, the number of coupled modes coincides with the number of chains within the unit cell. In case of PLLA, there are two chains in the unit cell and only in phase and out of phase coupling is possible, splitting each band in two components. The effect of intermolecular interactions is accounted for on going from column 2 to column 3, and the splitting associated is known as correlation (field) splitting, Davydov splitting, or exciton splitting.[22] The parallel A mode in the C_2 symmetry site correlates with the parallel B_1 mode in the D_2 symmetry of the unit cell of PLLA. The B modes of the two chains in the C_2 symmetry sites correlate with crystalline bands termed B_2 (in phase coupling) and B_3 (out of phase coupling). The overall effect resulting of going from column 1 to column 3 is termed Factor group splitting or Unit cell group splitting.[22] In case of PLLA, up to 10 possible vibrational modes can be expected.

The correlation table, Table 2, provides a general analysis, but the different splitting mechanisms are actually found in different scenarios. Site group splitting usually occurs when the symmetry of the site distorts the symmetry of the molecule, activating inactive modes for the single chain. This splitting is usually referred as crystal field splitting and the typical example is breaking the degeneracy of the degenerate X−O stretching modes in XO_4^{n-} anions.[32] Another possibility is found when molecules occupy more than one type of crystal site. This splitting mechanism is frequently found in inorganic molecules but is very unusual in organic crystals, probably because TDC interactions usually dominate over interactions between permanent dipoles in the absorption spectra. Davydov splitting (arising from TDC interactions) is not also a frequent result,[28] because strong enough dipole−dipole intermolecular interactions are necessary to couple the transition moments, but is the most commonly splitting mechanism encountered in organic crystals. As site splitting is very unusual in organic molecules, in most cases the overall splitting is simply due to correlation splitting or Davydov splitting, an the term factor group splitting is usually used as synonymous, even though it is not in the general case.[22]

C. Analysis of the Splitting in the C=O Stretching Region for the α-Crystals of PLLA. Site group splitting occurs due to the interaction between permanent dipoles. The classical expression for the static dipole−dipole interaction is[44]

$$V_{ij} = \frac{1}{4\pi\varepsilon_0\kappa}\frac{(\boldsymbol{\mu}_i\cdot\boldsymbol{\mu}_j) - 3(\boldsymbol{\mu}_i\cdot\mathbf{n}_{ij})(\boldsymbol{\mu}_j\cdot\mathbf{n}_{ij})}{{R_{ij}}^3} \quad (7)$$

where ε_0 is the electric permittivity of the vacuum, κ is the dielectric constant of the medium (κ = 3.8 for crystalline PLLA),[54] $\boldsymbol{\mu}$ is the dipole moment, $\mathbf{n}$ is the unit vector directed from the center of one dipole to the center of the other, and R_{ij} is the distance between the centers of dipoles in sites i and j.

In organic crystals, however, coupling is mainly governed by a mechanism governed by the transition dipole moment.[46] This mechanism was first proposed by Davydov to account for the splitting observed in the electronic spectra of molecular crystals, and later extended by Hexter to the analysis of vibrational bands.[46] According to this theory, during the absorption process the alternating electric field of light induces an alternating dipole in the absorbing vibrational mode, called transition dipole moment, which can couple through dipole−dipole interactions with another vicinal unperturbed vibrational mode. Coupling results in the transfer of excitation energy between the interacting groups, and this mechanism is also known as exciton coupling. The interaction energy obeys the form of eq 7 but replacing the static dipole moment by the transition dipole moment between states 0 and 1, $M = |<1|\boldsymbol{\mu}|0>|$, (where $\boldsymbol{\mu}$ is the dipole moment operator). Performing scalar products, the interaction energy arising from exciton interactions is:[44,46]

$$V_{ij} = \frac{|\langle 1|\mu|0\rangle|^2}{4\pi\varepsilon_0\kappa {R_{ij}}^3}[-2\cos\theta_i\cos\theta_j + \sin\theta_i\sin\theta_j\cos(\phi_i - \phi_j)] \quad (8)$$

where θ_i and θ_j are the angles that oscillators i and j subtend from the line between the centers, and ϕ_i and ϕ_j are the angles for the projections of oscillators i and j in the plane perpendicular to the line between the centers. The spectra of

Table 2. Wavenumbers for the Interactions in the Lateral Direction with C=O Groups Located in the First Layer Calculated According to the Atomic Coordinates of Aleman et al.[16] for the Five Different Sites Located along the PLLA Helix (See Spectrum in Figure 6).[a]

mode type	vibrational mode	30°	90°	150°	−150°	−90°	−30°	ΣK
in phase	I	1767.0	1765.5	1762.7	1760.8	1765.5	1763.6	4.78
	II	1778.4	1758.8	1755.0	1767.7	1758.8	1750.9	2.43
	III	1754.6	1758.8	1769.5	1753.1	1758.8	1773.3	2.11
	IV	1772.4	1747.9	1757.5	1764.2	1747.9	1752.9	−1.71
	V	1755.3	1747.9	1764.7	1757.6	1747.9	1768.3	−1.92
out of phase	VI	1751.0	1765.5	1755.3	1757.2	1765.5	1754.4	−0.78
	VII	1739.6	1758.8	1763.0	1750.3	1758.8	1767.1	−2.51
	VIII	1763.4	1758.8	1748.5	1764.9	1758.8	1744.7	−2.32
	IX	1745.6	1747.9	1760.5	1753.8	1747.9	1765.1	−5.11
	X	1762.7	1747.9	1753.3	1760.4	1747.9	1749.7	−4.97

[a] The angular terms indicate the angle subtended with the X axis by the line joining the centers of the helixes containing the interacting C=O groups (the direction shown in Figure 4 is 30°, remaining directions can be observed in Figure 3c). The vibrational modes of the different sites along the Z direction can be approximately characterized according to the schemes in Figure 5. Phase interactions with nonequivalent chains (located at ±30° and ±150° in Figure 3c) do not contribute to the spectrum.

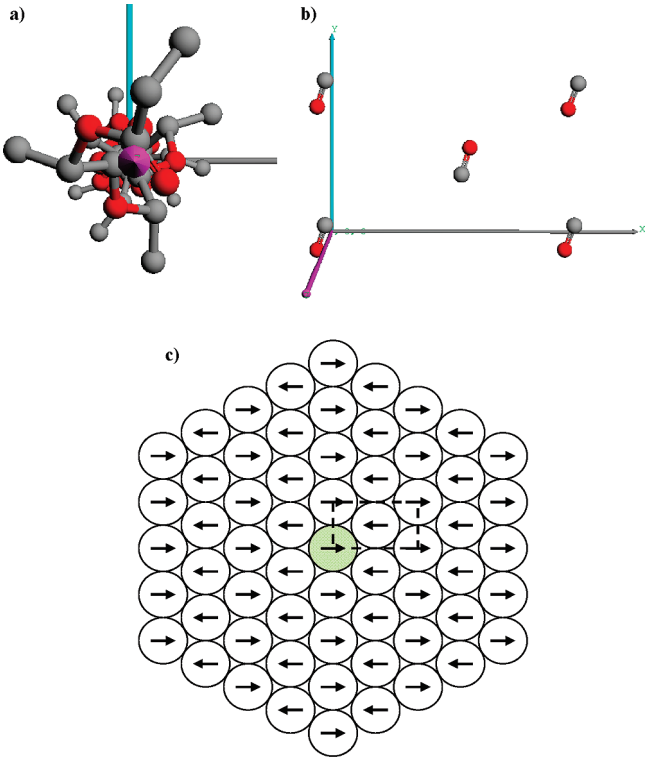

Figure 3. (a) Model of the crystalline 10_3 helix of PLLA according to the atomic coordinates of Aleman et al. (hydrogens are omitted for clarity). (b) Relative arrangement of the C=O groups located at an arbitrary site (same Z coordinate) in the α-crystal. (c) Simplified model of the α-crystal of PLLA. The arrows represent the perpendicular component of the transition moment for the C=O stretching mode.

proteins with known structure has been fairly well explained by Krimm et al. using amide I oscillators placed at the positions determined from the crystal structure and assuming that coupling occurs mainly through TDC interactions.[44,45] The through space interactions were considered a perturbation modifying the frequency of an isolated oscillator located at 1650 cm^{-1}.

The ester stretching vibration is highly localized in the C=O bond and TDC interactions occur between individual oscillators. At present, two sets of atomic coordinates can be used to locate the individual transition moments in the unit cell of PLLA; in the set of Aleman et al.[16] diffraction data were optimized against a regular helix model and in the set of Sasaki et al.[17] against a slightly distorted helix model. Figure 3a displays the regular helix model built using the coordinates of Aleman et al.[16] viewed along the *Z* axis direction. As can be seen, C=O groups are only slightly shifted from the center of the helix (distance between the center of the helix and the center of the dipole is 0.64 Å, compared to 6.1 Å between the centers of vicinal helixes). Figure 3b displays the projection in the *XY* plane of the C=O groups located in an arbitrary site (*Z* coordinate). As expected, C=O groups are approximately located in the center and in the corners of the unit cell. Splitting is expected to arise mainly from interactions with closest C=O groups, hence the location of farther C=O groups can be approximated. According to nearly circular profile for the 10_3 helix of PLLA viewed along the *Z* axis[19,54] and to the nearly hexagonal packing of chains in the α-crystals of PLLA,[6−9] the compact packing of rods (Figure 3c) can be an appropriate model to locate the relative arrangement of the chains in the α-crystals of PLLA. As discussed before, for distant chains the C=O groups can be approximately located in the center of the helixes, therefore the model shown in Figure 3c, containing the C=O groups (represented by arrows) in the center of the rod-like chains can be an appropriate model to compute distant interactions.

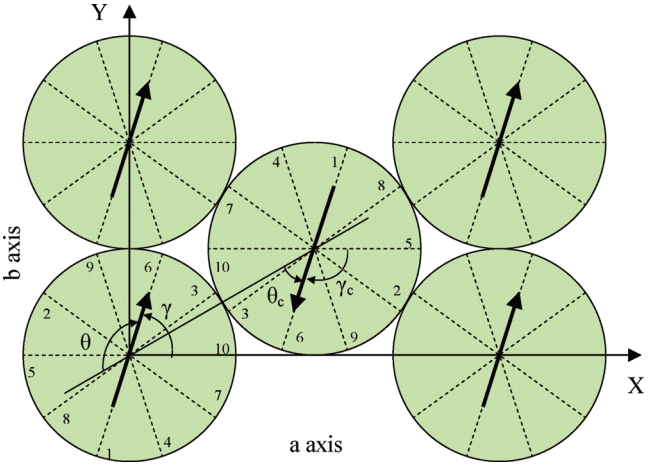

Figure 4. Schematic top view of the unit cell of PLLA in the $P2_12_12_1$ space group. The arrows indicate the perpendicular component of the transition moment for the in-phase vibrational mode of the site shown in Figure 3b, assuming that C=O groups are approximately located in the center of the helix. The numbers indicate the orientation of the C=O groups from bottom (no. 1) to top (no. 10) according to the the10_3 left handed helical structure of PLLA. The setting angle ω can be measured from the angle between the C=O group no. 10 and the X axis for the chain located in the origin (in this molecular model, $\omega = 0°$). Because of symmetry, the setting angle for the central chain is $\omega_c = \omega + 180°$. Angles θ and γ are defined as shown relative to the chain located in the origin. For the out of phase modes of the central helix, $\theta_c = \theta + 180°$ and $\gamma_c = \gamma + 180°$.

According to the correlation table, packing chains of C_{10} symmetry in sites of C_2 symmetry results in five distinguishable sites (the other five are rotated 180°). Recalling that TDC interactions are not observed in the *Z* direction for the α′-crystals, the sites are characterized exclusively by the lateral interactions (see also Figure 3b). Models for the remaining sites should be built using the atomic coordinates of the unit cell, but for the purposes of illustrating the vibrational modes of the sites, the simpler model shown in Figure 4 containing the C=O groups located in the centers of the helixes has been adopted. The dotted lines in Figure 4 indicate the direction for the C=O groups located at different heights along the chain according to the atomic coordinates of Aleman et al.[16] The rod-like chain is divided in sectors of 36°, and assuming that the transition moment is parallel to the C=O bond, the arrows represent the orientation of the transition moments. The direction for the first C=O bond, no. 1, has been arbitrarily set at 72° with the X axis, and the subsequent directions can be set rotating 108° counterclockwise according to the 10_3 left handed helical structure of PLLA. Carbonyl groups are therefore numbered from no. 1 to no. 10 from bottom to top of the unit cell. The orientation of the C=O groups (and therefore of the transition moment) for the chain in the corner of the unit cell can be obtained considering that PLLA crystallizes in the $P2_12_12_1$ space group characterized by two 2_1 screw axis in the directions of the a and b axes. Figure 5 displays the vibrational modes of the five distinguishable sites in the unit cell of PLLA. The B_2 modes (in phase vibrations relative to the symmetry of the unit cell) are I−V and the B_3 modes are VI−X. Compared to other well-known Davydov split bands such as those of polyethylene,[21] in case of PLLA total transition moments of the unit cell are no longer parallel to

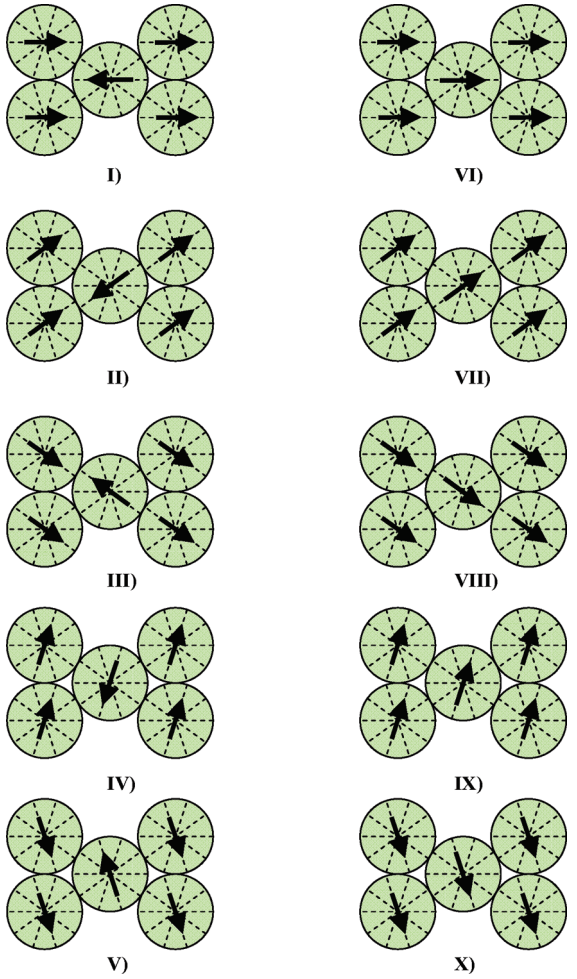

Figure 5. Vibrational modes for the sites in the unit cell of the α-crystal of PLLA. The arrows represent the perpendicular component of the total transition moment. The in phase B_2 modes are located to the left and the out of phase B_3 modes to the right.

the axes of the repetitive unit. This difference is due to different crystalline symmetries. Polyethylene crystallizes in the Pnam space group and due to the glide planes relating the chain in the center with the chain in the corner, B_2 and B_3 modes are parallel to the *b* and *a* axis of the unit cell respectively.[21]

The spectrum assuming lateral TDC interactions for the sites shown in Figure 5 can now be simulated. As only lateral interactions are considered (D_{0t} terms in Miyazawas treatment), the wavenumber can be calculated according to $\tilde{\nu} = 1759 \pm D_{0t}$. In Miyazawas treatment the positive sign is for in phase interactions ($\delta' = 0°$) and the negative sign for out of phase interactions ($\delta' = 180°$). Out of phase interactions do not contribute to the spectrum because the total transition moment is zero. Due to the arrangement of C═O groups in α-crystals (Figure 3b), D_{0t} terms depend on both distance and direction, and the interaction parameter for TDC interactions can be calculated according to $D = V/hc$ where *V* is the interaction energy (eq 8), *h* is Planck's constant, and *c* is the speed of light;[44] therefore:

$$\tilde{\nu}_{ij} = 1759 + \frac{M^2}{4\pi\varepsilon_0 \kappa hcb^3}(-2\cos\theta_i \cos\theta_j + \sin\theta_i \sin\theta_j)\left(\frac{6.1}{d_{ij}}\right)^3 \quad (9)$$

where the unperturbed frequency for the crystalline gt conformers is $\tilde{\nu}_0 = 1759\ \mathrm{cm}^{-1}$, $b = 6.1 \times 10^{-10}$ m (length of the *b* axis), and d_{ij} is the distance between the interacting chains measured in Angstroms. Equation 9 can be shortened to $\tilde{\nu}_{ij} = 1759 + CK_{ij}$, where *C* is the constant ratio in the right-hand side and K_{ij} is a geometric factor depending on θ and d_{ij}.

The intensity of vibrational modes is proportional to the square of the transition moment. The square of the transition moment for the interacting pair can be calculated as the vector sum of the squares of the individual transition moments.[44] In addition, a factor accounting for the lower probability of the interaction at larger distances must be introduced; therefore:

$$I_{ij} = (1+\cos(\theta_i - \theta_j))\left(\frac{6.1}{d_{ij}}\right)^3 \quad (10)$$

Finally, the spectrum can be simulated assuming a Gaussian profile for each component according to:

$$A_{ij} = \left(\frac{4\ln 2}{\pi}\right)^{1/2} \frac{I_{ij}}{w_h} \exp\left(-(4\ln 2)\left(\frac{\tilde{\nu}_{ij} - 1759}{w_h}\right)^2\right) \quad (11)$$

Here A_{ij} is the absorbance, I_{ij} is the intensity (integrated absorbance) of the peak, and w_h is the full width at half-height.

The K_{ij} values of eq 9 have been calculated for the five sites vibrating in phase and out of phase and assuming only lateral interaction. For a particular site (such as that of Figure 3b), the coordinates of Aleman et al. have been exclusively used to compute the interactions with the first layer; interactions with the remaining layers have been approximately calculated assuming that C═O groups are located in the centers of the respective helixes (Figure 3c). Once all the K_{ij} values have been obtained up to the fourth layer, $\tilde{\nu}_{ij}$ values are obtained assuming a fitting value for *C* in eq 9. The calculated wavenumbers with the corresponding intensities (eq 10) are substituted in eq 11, where a single width is assumed. The simulated spectrum is the sum of all the calculated components. Simulation of the spectrum using eqs 9, 10, and 11 depends mainly on the parameter C. The effect of w_h is secondary because it varies in a restricted range ($5-6\ \mathrm{cm}^{-1}$) and does not actually affect the degree of splitting or the relative intensities.

Figure 6 shows the spectrum simulated for the α-crystals of PLLA using the atomic coordinates of Aleman et al.[16] The contribution corresponding to the B_1 parallel band at $1776\ \mathrm{cm}^{-1}$ is not observed in the simulated spectrum because only perpendicular contributions have been considered. The location of the individual contributions for the interactions with the chains located in the first layer is listed in Table 2. As can be seen, the experimental C═O stretching band can be regarded as a continuum of adjacent contributions, from which only the overall envelope is observed. The experimental spectrum is fairly well simulated regarding the shapes of the absorbance spectrum and the second derivative. Most of the splitting is due to interactions with chains located in the first layer. Interactions with equivalent chains (located at ± 90°, *b* axis) show higher symmetry than interactions with nonequivalent chains. For the former, the distance between the centers of the interacting dipoles is always 6.1 Å, and because $\omega \approx 0°$ (see Figure 4) modes II and III and modes IV and V present identical K_{ij} values. As a consequence, interactions between equivalent chains occur only at certain wavenumbers (about $1766\ \mathrm{cm}^{-1}$ for site I; $1759\ \mathrm{cm}^{-1}$ for sites II and III and $1748\ \mathrm{cm}^{-1}$ for sites IV and V), being therefore the main responsible for the apparent contributions observed

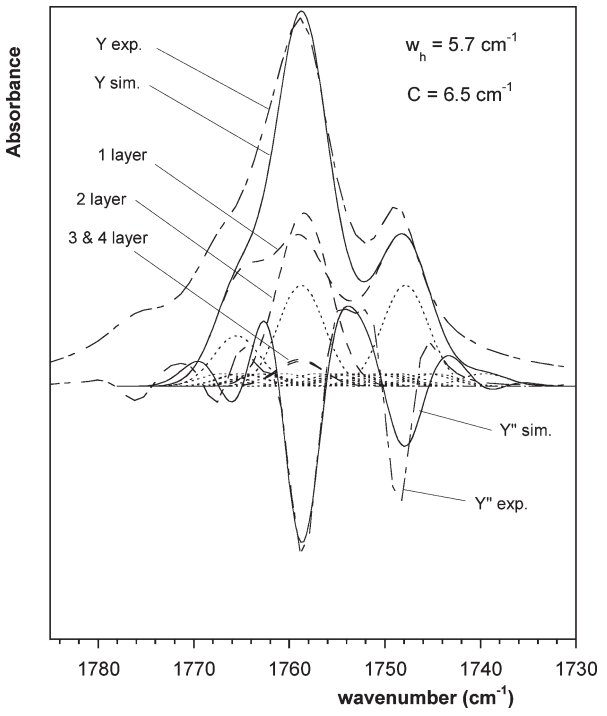

Figure 6. Comparison of the spectrum simulated for the crystalline structure of α-crystals of PLLA according to the coordinates of Aleman et al.[16] with the experimental spectrum. Continuous line: simulated spectrum; short dashed lines: contributions for the interactions with the first layer; normal dashed lines: total contributions corresponding to the interactions with different layers; long dashed lines: experimental spectrum (crystallinity 80%).

at about those locations in the second derivative spectrum. Interactions with chains located farther only contribute to the central part of the peak.

Although it is commonly accepted that in organic crystals Davydov splitting usually accounts for most (if not all) of the splitting, the possibility of site group splitting has also been analyzed. The split of permanent dipoles follows eq 7 (or eq 8 replacing the transition moment by the dipole moment). Models I−V in Figure 5 represent the location of the permanent dipole moments in the approximate model assuming C═O groups located in the center of the helix. The split corresponding to each site can be calculated according to:

$$\tilde{\nu}_S = 1759 + \frac{\mu^2}{4\pi\varepsilon_0 \kappa hcb^3} \sum_{ij} (-2 \cos\theta_i \cos\theta_j + \sin\theta_i \sin\theta_j) \left(\frac{6.1}{d_{ij}}\right)^3 \quad (12)$$

Here $\tilde{\nu}_S$ is the split frequency of site S and the sumation represents the geometric factor for the interaction with all the permanent dipoles in the crystal. Equation 12 has been used to simulate possible frequency shifts for the different sites assuming arbitrary fitting values for the quotient in the right-hand side, but any fitting attempt gives poor results. In summary, site splitting is not observed, and the profile of the C═O stretching band can be explained assuming exclusively transition dipole coupling (Davydov splitting) of the five unperturbed sites located along the unit cell.

From the value of the fitting constant $C = 6.5\ \text{cm}^{-1}$, the perpendicular component of the transition moment obtained from eq 9 is 1.06 D, and considering the angle between the C═O groups and the +Z axis,[16] 79.1°, the transition moment is M = 1.07 D. In the approximation of the harmonic oscillator,[44] the dipole moment derivative can be calculated according to

$$M = \frac{\partial\mu}{\partial Q}\left(\frac{h}{8\pi^2\tilde{\nu}c}\right) \quad (13)$$

using $\tilde{\nu} = 1759\ \text{cm}^{-1}$, $\partial\mu/\partial Q = 10.94\ \text{D Å}^{-1}\ \text{u}^{-0.5}$ is obtained. This value is about five times the typical derivative value for ester groups.[47] In case of the model compound 2-methoxymethylpropanoate,[19] a value $\partial\mu/\partial Q = 2.20\ \text{D Å}^{-1}\ \text{u}^{-0.5}$ has been reported, in good agreement with the fifth part of our result (10.94/5 = 2.19). The dynamics of exciton interactions are at present a research subject, but the existence of collective excitonic modes in systems with attractive TDC interactions has been extensively reported.[48−50] In these collective modes, the absorption of a single photon drives a concerted multiexciton transfer occurring on several nearby molecules.[48] Therefore, a collective interaction involving the five distinguishable C═O groups in PLLA seems to be the origin for the strong splitting observed in the C═O stretching region of crystalline polylactides.

Simulating the spectra using accurate atomic coordinates is somewhat cumbersome. A simpler model containing all the C═O groups in the center of the helix would simplify the task of extending the analysis of the C═O stretching band to other hypothetical crystals, providing the opportunity to test the sensitivity of TDC interactions to crystalline structure. Figure 7a is the simulated spectrum of PLLA assuming that all C═O groups are be located in the centers of the helixes. As can be seen, the spectrum is very similar to that calculated using the atomic coordinates of Aleman et al.,[16] suggesting that the slight change in coordinates between the two models has a minor effect. Therefore, the model of Figure 3c, containing all the C═O groups located in the center of the helix will be used to simulate the spectra of hypothetical crystals. The setting angle, ω, is defined as the rotation angle of the helix relative to the arrangement corresponding to α-crystals (Figure 4). Assuming crystallization in the $P2_12_12_1$ space group, the setting angle for the central chain is $\omega_c = \omega + 180°$. The spectrum simulated with $\omega = 36°$ is identical to the spectrum with $\omega = 0°$ as both structures contain C═O groups parallel to the *a* axis; actually the simulated spectra are symmetrical around $\omega = 18°$ (arrangement containing C═O groups parallel to the *b* axis). Parts a, c, and d of Figure 7 show the spectra simulated for different crystals with setting angles covering the range 0−18°. As can be seen the spectra change noticeably with the setting angle (with the angular arrangement of transition moments). The experimental spectrum is clearly incompatible with the arrangements in which the C═O groups can be oriented parallel to the *b* axis.

Sasaki et al.[17] have proposed a slightly distorted helix structure in which C═O groups are oriented at γ = 5.9, 36.6, −33.2, 76.3, and 71.1° (γ is defined in Figure 4) and the mean distance between the C═O groups and the helix axis (0.47 Å) is smaller than that of the helix of Aleman et al.[16] Although the orientation of the C═O groups within the unit cell seems not so different from that corresponding to the regular helix with $\omega = 0°$, the spectrum has been calculated assuming again the simplification of locating all the C═O groups in the centers of the helixes. As can be seen (Figure 7b), the new orientations for the C═O groups improve slightly the fitting to the experimental spectrum. Specifically, the skewness to higher wavenumbers observed for the second derivative contribution at about 1749 cm^{-1} calculated according to the atomic coordinates of Aleman et al. is now slightly reduced. Anyway, the crystalline structures proposed by Aleman and by Sasaki are not so different and the improvement is small.

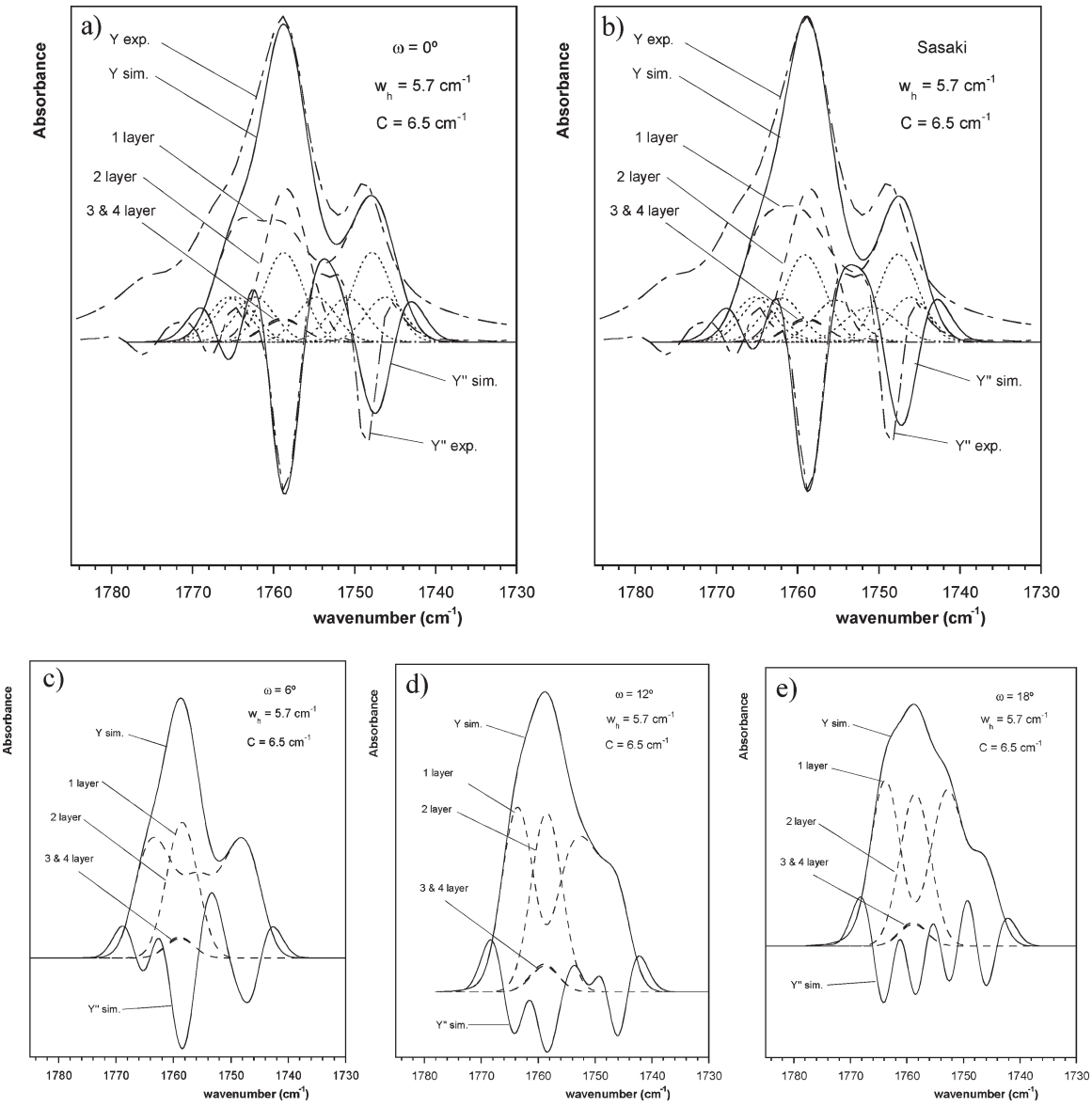

Figure 7. (a) Spectrum of PLLA simulated assuming that all C=O groups are located in the center of the helixes and $\omega = 0°$. (b) Spectrum of PLLA simulated assuming that all C=O groups are located in the center of the helixes and using the orientation of C=O groups obtained by Sasaki et al.[17] (c–e) Spectra predicted for hypothetical crystalline forms of PLLA, characterized by different setting angles, ω, assuming crystallization in the $P2_12_12_1$ space group.

The analysis of TDC interactions also allows an estimation of the strength of dipole–dipole interactions. In the five different sites identified along the Z axis, permanent dipoles can be oriented according to modes I–V of Figure 5. As can be seen, dipoles located in nonequivalent chains show a head to head arrangement, suggesting repulsive interactions. The total value of K corresponding to the interactions with chains in the first layer for the permanent dipoles (Table 2) in the five different sites is K=5.69. Successive layers can contribute with attractive or repulsive interactions (see table 3), but the total value K=5.13 for the first four layers stands close to the value calculated for the first layer. Neglecting interactions above the fourth layer and assuming a typical dipole moment of 2.5 D for the ester group,[51] the strength of the repulsive dipole–dipole interactions is estimated about 0.5 kJ/mol.

Aleman et al.[16] also reported that repulsive interactions pulling apart the PLLA chains could be readily observed during Montecarlo simulations. The main intermolecular interactions expected in the chain packing of PLLA are dispersive interactions and dipole–dipole interactions. The former are usually stronger because they are established over a wide contact surface. In fact, dipole–dipole interactions are not considered a factor determining crystalline structures,[52] and the typical strength of these interactions in systems with favorable (attractive) molecular arrangements is usually small, of about 2 kJ/mol.[53] The strength of dispersive interactions is variable, depending on several factors such as molecular size or spatial matching. The

Table 3. Values of the Geometric Factor for the Lateral Interactions between Permanent Dipoles in Sites I–V, Computed up to the Fourth Layer[a]

layer	ΣK
1	5.69
2	−0.91
3	0.73
4	−0.38
total	5.13

[a] The total value is positive, and the strength of repulsive interactions is about 0.5 kJ/mol.

Table 4. Values of the Total Geometric Factor for the Lateral Interaction between C=O Dipoles Computed up to the Fourth Layer for Different Setting Angles (ω)[a]

ω (deg)	ΣK
0	4.44
18	1.80
36	−5.11
54	−13.6
72	−20.5
90	−23.2

[a] The value of ΣK for the arrangement with $\omega = 0°$ differs from that of Table 3 because the simplified model, containing all C=O groups in the center of the helix, has been adopted in this calculation. If the setting angle is rotated 90°, permanent dipoles would become arranged in parallel orientation, resulting in attractive interactions of about −2.0 kJ/mol.

overall effect of these interactions is always attractive and depends strongly on distance according to R^{-6}. Therefore, dispersive interactions will always dominate over dipole−dipole interactions at short distances but may not at larger distances, because the distance dependence of the latter is smoother (R^{-3}). The repulsive interactions observed by Aleman et al.[16] agree with the repulsive dipole−dipole interactions found in this study.

The value of the geometric factor K for the interactions between permanent dipoles with the first four layers has also been computed for values of ω between 0° and 90° (see Table 4) In this case, data are symmetrical around 90° because 0° means permanent dipoles arranged according to B_2 modes of Figure 5 and 90° means permanent dipoles arranged as the B_3 modes. As expected from the simple visual inspection of the modes in Figure 5, values of K in table 4 decrease as the permanent dipoles rotate to arrange in parallel orientation. The value of K is positive in the range 0−24° and negative (attractive interactions) in the range 24−90°. If PLLA would crystallize in the arrangement with $\omega = 90°$ ($K = -23.2$ for five sites) the strength of dipole−dipole interactions would be $\Delta E = -2$ kJ/mol, in nice agreement with the typical value for systems in which favorable dipole−dipole orientation occurs.

Finally, some aspects of the parallel band at 1777 cm^{-1} deserve a final comment. One of them is the absence of this band in the α′ crystal although it is present in the α crystal. Because of its higher regularity, the sample crystallized in the α-form (Figure 2a) shows a higher crystallinity degree than the sample crystallized in the α′-form (80% versus 46%). Therefore, in the former sample there is only 20% of amorphous sample versus 54% in the latter. This difference in crystalline/amorphous contents between the two crystalline polymorphs should decrease the resolution of the crystalline components for the α′-form, difficulting band distinguishing. Overall, the spectrum of the α′-form always shows broader, less resolved peaks, probably due to the combination of lower order in the crystalline phase (broader peaks) and to higher amorphous contents. It is therefore difficult to ensure whether the absence of the band at 1776 cm^{-1} in the α′-form is due to its absence or to the lack of resolution. Also, even though both polymorphs crystallize in a 10_3 helix, they show slightly different X-ray diffractograms, and atomic coordinates should differ. This factor may additionally act reducing the inherent intensity of the A mode in the α′-form. The other aspect deserving a specific comment is that this band (1776 cm^{-1}) is not shifted by TDC interactions in the α crystals even though the geometric factor is not zero for vicinal dipoles in parallel orientation. TDC splitting is proportional to the square of the transition moment (eq 8), or to the intensity of the band, and in bands of low intensity TDC splitting is also small. This is a known property of TDC interactions.[44]

Conclusions

The C=O stretching region for the α-crystals of PLLA has been analyzed. The band at 1776 cm^{-1} arises from the parallel component of the transition moment. For this component, TDC interactions are negligible due to its small transition moment and the location of the band is attributed to the through bond coupling interaction (eq 3, $\delta = 0°$). The absorption profile observed below this wavenumber is attributed to coupling of transition moments (Davydov splitting) in the lateral direction. The arrangement of transition moments in the lateral direction allows the identification of five different sites along the PLLA helix in the unit cell, each of them establishing different interactions with the vicinal chains located in the first layer. Site splitting due to interaction between permanent dipoles is not observed, and the spectrum can be reproduced considering Davydov splitting around the same central location (1759 cm^{-1}) for all the sites. The perpendicular absorptions are highly overlapped and the C=O stretching band can be regarded as a continuum of adjacent contributions, from which only the overall envelope is observed, containing three apparent components located at 1767, 1759, and 1749 cm^{-1}. The latter has been related to α-crystals, but actually all the profile should be related to these crystals. The value obtained for the transition moment suggests that excitonic interactions may occur in a collective mode involving the five distinguishable C=O groups in PLLA, explaining the large splitting observed in the C=O stretching region of crystalline polylactides.

The analysis of intermolecular interactions reveals repulsive dipole−dipole interactions of about 0.5 kJ/mol. The origin of the repulsive interaction is best understood observing Figure 4. Carbonyl groups between chains in antiparallel orientation are oriented head to head (repulsive interactions, see for example C=O groups no. 3, no. 7, no. 2, no. 8). However carbonyl groups between chains in parallel orientation are oriented head to tail (attractive interactions). In the hexagonal packing, PLLA chains are surrounded by four chains in antiparallel orientation (the four chains located in the corners of the unit cell) and two chains with parallel orientation. Therefore, the number of repulsive interactions exceeds the number of attractive interactions. As the relative arrangement of C=O groups is a consequence of the symmetry of the repetitive unit, the repulsive interactions is related to the symmetry of the unit cell ($P2_12_12_1$ space group).

Acknowledgment. The authors are thankful for financial support from the Basque Government Dept.of Education, University and Research (consolidated research groups GIC07/136-IT-339-07) and from Spanish Ministerio de Ciencia y Tecnología with Project MAT 2006-13436-C02-01. They would also like to acknowledge the collaboration of other members of CIC biomaGUNE and the support from the *Biobask* Agency (Project Etortek IE07-201).

References and Notes

(1) Martina, M.; Hutmacher, D. W. *Polym. Int.* **2007**, *56*, 145–157.
(2) Auras, R.; Harte, B.; Selke, S. *Macromol. Biosci.* **2004**, *4*, 835–864.
(3) De Santis, P.; Kovacs, A. J. *Biopolymers* **1968**, *6*, 299–306.
(4) Eling, B.; Gogolewski, S.; Pennings, A. J. *Polymer* **1982**, *23*, 1587–1593.
(5) Cartier, L.; Okihara, T.; Ikada, Y.; Tsuji, H.; Puiggali, J.; Lotz, B. *Polymer* **2000**, *41*, 8909–8919.
(6) Iwata, T.; Doi, Y. *Macromolecules* **2000**, *33*, 5559–5565.
(7) Hoogsteen, W.; Postema, A. R.; Pennings, A. J.; ten Brinke, G.; Zugenmaier, P. *Macromolecules* **1990**, *23*, 634–642.
(8) Kalb, B.; Pennings, A. J. *Polymer* **1980**, *21*, 607–612.

(9) Kikkawa, Y.; Abe, H.; Fujita, M.; Iwata, T.; Inoue, Y.; Doi, Y. *Macromol. Chem. Phys.* **2003**, *204*, 1822–1831.
(10) Ohtani, Y.; Okumura, K.; Kawaguchi, A. *J. Macromol. Sci., Part B: Phys.* **2003**, *42*, 875–888.
(11) Yasuniwa, M.; Tsubakihara, S.; Iura, K.; Ono, Y.; Dan, Y.; Takahashi, K. *Polymer* **2006**, *47*, 7554–7563.
(12) Zhang, J.; Duan, Y.; Sato, H.; Tsuji, H.; Noda, I.; Yan, S.; Ozaki, Y. *Macromolecules* **2005**, *38*, 8012–8021.
(13) Takahashi, K.; Sawai, D.; Yokoyama, T.; Kanamoto, T.; Hyon, S. H. *Polymer* **2004**, *45*, 4969–4976.
(14) Sawai, D.; Takahashi, K.; Sasashige, A.; Kanamoto, T.; Hyon, S. H. *Macromolecules* **2003**, *36*, 3601–3605.
(15) Zhang, J.; Tashiro, K.; Tsuji, H.; Domb, A. J. *Macromolecules* **2007**, *40*, 1049–1054.
(16) Aleman, C.; Lotz, B.; Puiggali, J. *Macromolecules* **2001**, *34*, 4795–4801.
(17) Sasaki, S.; Asakura, T. *Macromolecules* **2003**, *36*, 8385–8390.
(18) Kawai, T.; Rahman, N.; Matsuba, G.; Nishida, K.; Kanaya, T.; Nakano, M.; Okamoto, H.; Kawada, J.; Usuki, A.; Honma, N.; Nakajima, K.; Matsuda, M. *Macromolecules* **2007**, *40*, 9463–9469.
(19) Aou, K.; Hsu, S. L. *Macromolecules* **2006**, *39*, 3337–3344.
(20) Lagaron, J. M. *Macromol. Symp.* **2002**, *184*, 19–36.
(21) Bower, D. I.; Maddams, W. F. in *The Vibrational Spectroscopy of Polymers*; Cambridge University Press: Cambridge, U.K., 1989.
(22) Bertie, J. E. in *Handbook of Vibrational Spectroscopy, Vol. 5: Glossary of Terms Used in Vibrational Spectroscopy*; Chalmers, J., Griffiths, P., Eds.; John Wiley & Sons, Ltd.: Chichester, U.K., 2002.
(23) Schindler, A.; Harper, D. H. *J. Polym. Sci., Polym. Chem. Ed.* **1979**, *17*, 2593–2599.
(24) Meaurio, E.; López-Rodríguez, N.; Sarasua, J. R. *Macromolecules* **2006**, *39*, 9291–9301.
(25) Kister, G.; Cassanas, G.; Vert, M. *Polymer* **1998**, *39*, 267–273.
(26) Zhang, J.; Tsuji, H.; Noda, I.; Ozaki, Y. *J. Phys Chem. B* **2004**, *108*, 11514–11520.
(27) Meaurio, E.; Zuza, E.; Sarasua, J. R. *Macromolecules* **2005**, *38*, 1207–1215.
(28) Painter, P. C.; Coleman, M. M.; Koenig, J. L. in *The Theory of Vibrational Spectroscopy and its Applications to Polymeric Materials*; John Wiley & Sons: New York, 1982.
(29) Kang, S.; Hsu, S. L.; Stidham, H. D.; Smith, P. B.; Leugers, M. A.; Yang, X. *Macromolecules* **2001**, *34*, 4542–4548.
(30) Heidberg, J.; Hustedt, M.; Kampshoff, E.; Rozenbaum, V. M. *Surf. Sci.* **1999**, *427−8*, 431–438.
(31) Ouasri, A.; Rhandour, A.; Dhamelincourt, M. C.; Dhamelincourt, P.; Mazzah, A. *J. Raman Spectrosc.* **2002**, *33*, 726–729.
(32) Lutz, H. D.; Haeuseler, H. *J. Mol. Struct.* **1999**, *511−2*, 69–75.
(33) Meaurio, E.; Zuza, E.; López-Rodríguez, N.; Sarasua, J. R. *J. Phys. Chem. B* **2006**, *110*, 5790–5800.
(34) Sarasua, J. R.; López-Rodríguez, N.; López-Arraiza, A.; Meaurio, E. *Macromolecules* **2005**, *38*, 8362–8371.
(35) Krimm, S.; Abe, Y. *Proc. Natl. Acad. Sci. U.S.A.* **1972**, *69*, 2788–2792.
(36) Painter, P. C.; Pehlert, G. J.; Hu, Y.; Coleman, M. M. *Macromolecules* **1999**, *32*, 2055–2057.
(37) Torii, H.; Tasumi, M. *J. Raman Spectrosc.* **1998**, *29*, 81–86.
(38) Besley, N. A.; Metcalf, K. A. *J. Chem. Phys.* **2007**, *126*, 35101–7.
(39) Torii, H. *J. Phys. Chem.* **2004**, *108*, 7272–7280.
(40) Gorbunov, R. D.; Stock, G. *Chem. Phys. Lett.* **2007**, *437*, 272–276.
(41) Hayashi, T.; Mukamel, S. *J. Mol. Liq.* **2008**, *141*, 149–154.
(42) Popov, E. M.; Khomenko, A.Kh.; Shorygin, P. P. *Izv. Akad. Nauk SSSR, Ser. Khim.* **1965**, *1*, 51–58.
(43) Brant, D. A.; Tonelli, A. E.; Flory, P. J. *Macromolecules* **1969**, *2*, 228–235.
(44) Barth, A.; Zscherp, C. *Q. Rev. Biophys.* **2002**, *35*, 369–430.
(45) Krimm, S.; Bandekar, J. *Adv. Protein Chem.* **1986**, *38*, 181–364.
(46) Giorgini, M. G. *Pure Appl. Chem.* **2004**, *76*, 157–169.
(47) Galabov, B.; Bovadova-Parvanova, P.; Dudev, T. *J. Mol. Struct.* **1997**, *406*, 119–125.
(48) Painelli, A.; Terenziani, F. *Synth. Met.* **2004**, *147*, 111–115.
(49) Scholes, G. D.; Rumbles, G. *Nat. Mat* **2006**, *5*, 683–696.
(50) Gao, B. L.; Xiong, Y.; Xiong, S. J. *Phys. Rev. B* **2006**, *74*, 235102(5).
(51) Israelachvili, J. N. *Intermolecular & Surface Forces*; Academic Press: Amsterdam, 1992.
(52) Lee, S.; Mallik, A. B.; Fredrickson, D. C. *Cryst. Growth Des.* **2004**, *4*, 279–290.
(53) Atkins, P. W. *Physical Chemistry*, 6th ed.; Oxford University Press: Oxford, U.K., 1998.
(54) Nakagawa, T.; Nakiri, T.; Hosoya, R.; Tajitsu, Y. *IEEE Trans. Ind. Appl.* **2004**, *40*, 1020–1024.
(55) Beaucage, G.; Rane, S.; Sukumaran, S.; Satkowski, M. M.; Schechtman, L. A.; Doi, Y. *Macromolecules* **1997**, *30*, 4158–4162.